



# Evidence of site amplification from ground motion of the last two large crustal earthquakes in central-western Argentina

Patricia Alvarado<sup>1,2</sup> · Rodolfo Christiansen<sup>3,4</sup> · Salvador Daniel Gregori<sup>2,3</sup> · Mauro Saez<sup>1,2</sup>

Received: 23 March 2019 / Accepted: 17 April 2020 / Published online: 28 April 2020  
© Springer Nature B.V. 2020

## Abstract

The present study has investigated site amplification effects from the analysis of peak ground accelerations (PGA) and spectral accelerations (SA) of the last two major crustal earthquakes in central-western Argentina. These data were obtained from 15 accelerometers and 57 seismoscopes, which recorded ground motions during the 1977 ( $M_w$  7.5) San Juan earthquake, and the 1985 ( $M_w$  5.9) Mendoza earthquake. PGA and SA measurements were compared with average values predicted by global attenuation empirical relationships for the same type of crustal earthquakes. The amplifications in ground accelerations were analyzed according to their distribution and compared with the average shear wave velocities at 30 m depth ( $V_{s30}$ ) where the stations are located. Our results definitively show that site effects and direction of maximum surface wave radiation strongly amplify the ground acceleration during moderate to large earthquakes near San Juan and Mendoza (Argentina); this is of importance in seismic hazard analyses.

**Keywords** Seismic hazard · Peak ground acceleration · Spectral acceleration · Surface wave radiation pattern

---

✉ Rodolfo Christiansen  
rodolfo.christiansen@conicet.gov.ar

Patricia Alvarado  
alvarado@unsj.edu.ar

<sup>1</sup> Centro de Investigaciones de la Geósfera y Biósfera CIGEOBIO (CONICET-Universidad Nacional de San Juan UNSJ), Av. Ignacio de la Roza 590, CP: J5402DCS Rivadavia, San Juan, Argentina

<sup>2</sup> Departamento de Geofísica y Astronomía - FCEfYn, Universidad Nacional de San Juan, San Juan, Argentina

<sup>3</sup> Instituto Geofísico Sismológico Volponi (IGSV) - FCEfYn, Universidad Nacional de San Juan, 5407 Rivadavia, San Juan, Argentina

<sup>4</sup> Consejo Nacional de Investigaciones Científicas y Técnicas (CONICET), CCT San Juan, Argentina

## 1 Introduction

Every detailed evaluation of the seismic hazard for a particular region involves attenuation relationships, which consider parameters of engineering interest, such as seismic intensity, peak ground acceleration (PGA) and spectral acceleration (SA). This practice necessarily assumes having an adequate number of records of the larger earthquakes obtained from strong motion instruments appropriately distributed over a study area. The central-western part of Argentina is recognized as the region exposed to the greatest occurrence of earthquakes and of greater magnitudes in this country (Gregori 1993; Alvarado and Araujo 2011; Gregori and Christiansen 2018) (Fig. 1). In this region a significant seismic activity, sometimes causing severe damage, is observed within the continental crust of the South American Plate with focal depths <35 km (e.g. United States Geological Survey earthquake catalog). The subducting Nazca Plate also exhibits 100 to 200 km intermediate-depth earthquakes beneath densely populated areas (Alvarado and Araujo 2011) but their maximum seismic intensities are comparatively lower than those of crustal earthquakes. Recorded acceleration data from large earthquakes are very scarce in this region making difficult to obtain an estimation of the ground acceleration attenuation with distance. In this study, acceleration data for the last two major reverse-fault crustal earthquakes in central western Argentina are compared to global data for other active tectonic regions. The aim of this study is to understand the attenuation of ground acceleration with distance and describe site amplification for this hazardous region.

Several analog accelerometers capable of detecting the variation of ground accelerations have recorded the 1977 ( $M_w$  7.5) San Juan and 1985 ( $M_w$  5.9) Mendoza earthquakes of Argentina (Fig. 2). These instruments were deployed and maintained since 1962 by the Instituto de Investigaciones Antisísmicas Ing. Aldo Bruschi of the Universidad Nacional de San Juan, and the Instituto Nacional de Prevención Sísmica (INPRES). Four accelerometer records were analyzed for the 1977 earthquake (Table 1) and 11 for the 1985 earthquake (Table 2). In addition, 39 seismoscope records of the 1977 earthquake (Table 3) and 18 of the 1985 earthquake (Table 4) were analyzed. Paper records from the accelerometers were digitized in order to estimate the Peak Ground Accelerations (PGA) using the maximum amplitude of the recorded seismic waves. These records did not show amplitude saturation in comparison to those from local seismometers. In addition, information from the seismoscopes was examined to obtain spectral accelerations (SA).

It is worth to note that the strong motion acceleration records here studied represent the first instrumental records of large earthquakes in Argentina. These records are compared with the global empirical attenuation relationships of Abrahamson and Silva (1997, 2008) and Sadigh et al. (1997) for soil and rock. The main goal was to analyze their predictability for the 1977 and 1985 crustal earthquake motions. The results are discussed in terms of site amplifications considering surface-wave radiation patterns for both seismic events. These values are also compared in a framework of regional-scale information of average shear-wave velocities at 30 m depth ( $V_{s30}$ ).

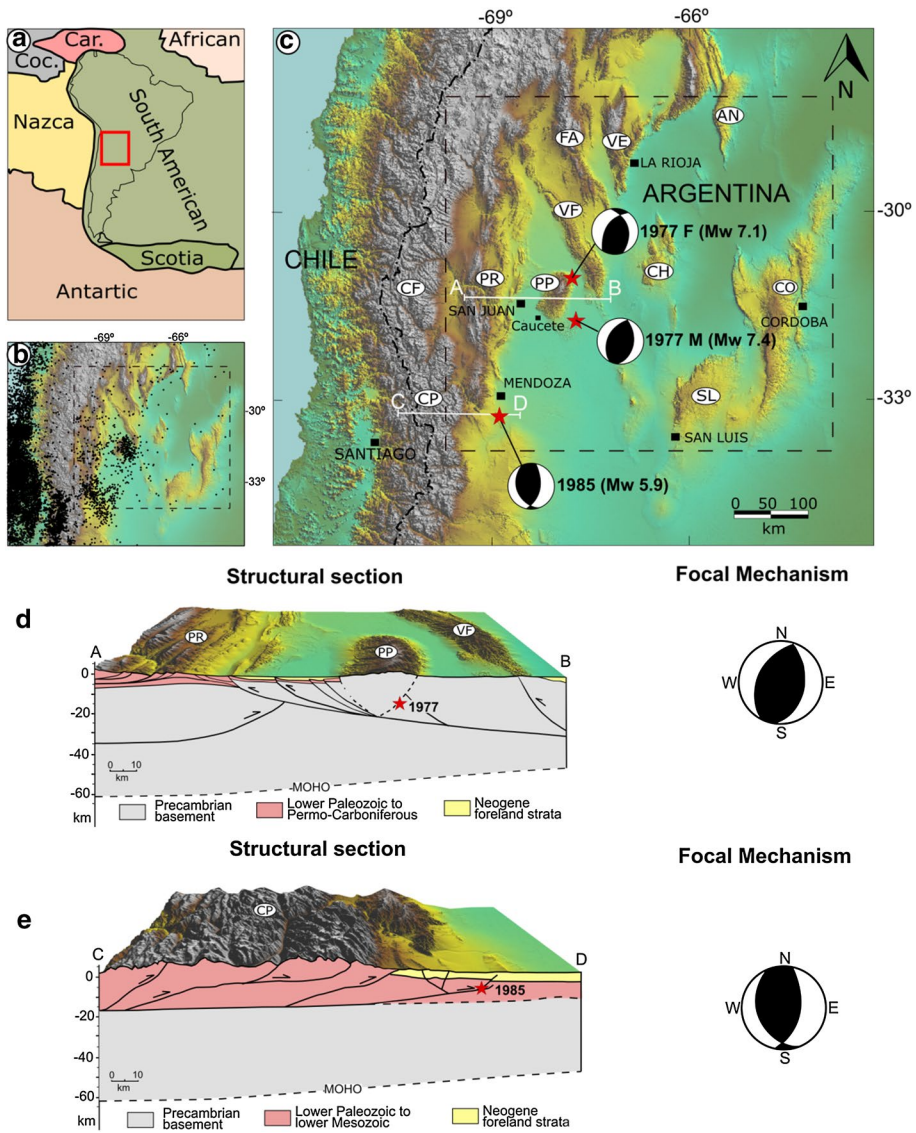


**Fig. 1** a Plate tectonic configuration and location of the studied area (red rectangle) in the context of South America. Coc: Cocos Plate, Car: Caribbean Plate. **b** Epicentral distribution of shallow seismic events ( $M_w > 3.5$ ) from 1575 to 2017 according to the USGS (2018). **c** Dashed line rectangle represents the study area and black squares the main cities. CP Cordillera Principal, SL Sierra de San Luis, CO Sierras de Córdoba, PP Sierra de Pie de Palo, PR Precordillera, CF Cordillera Frontal, VF Sierra de Valle Fértil, CH Sierra de Chepes, AN Sierra de Ancasti, VE Sierra de Velasco, FA Sistema de Famatina. **d** 3D-view, schematic cross-section A–B at  $-31.45^\circ$  and focal mechanism for the 1977 San Juan multiple earthquake. F Foreshock, M Mainshock, **e** 3D-view, schematic cross-section C–D at  $-33.11^\circ$  and focal mechanism for the 1985 Mendoza earthquake ( Modified from Chiamonte et al. 2000; Alvarado and Beck 2006) (Seismic source data from the CMT Project catalog, Ekström et al. 2012)

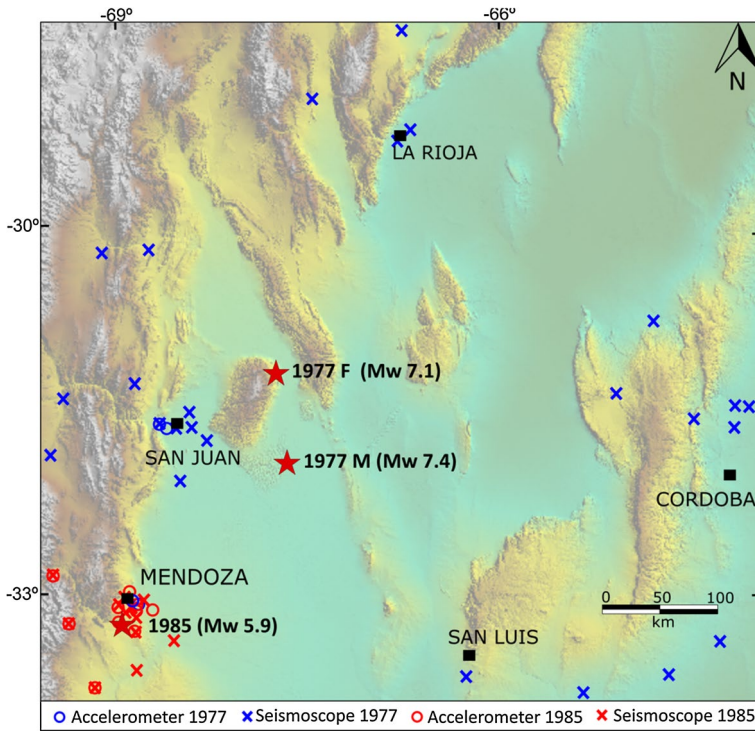


**Fig. 2** Location of 4 accelerometers (blue circles) and 39 seismoscopes (blue crosses) which provided data for the 1977 ( $M_w$  7.5) San Juan earthquake. Location of 11 accelerometers (red circles) and 18 seismoscopes (red crosses) which provided data for 1985 ( $M_w$  5.9) Mendoza earthquake

**Table 1** Maximum accelerations (PGA) recorded during the 1977 ( $M_w$  7.5) San Juan earthquake for four instruments showing their locations (first three columns), component, Peak Ground Accelerations PGA and distance to the epicenter  $R_{rup}$

Province	Locality	Site	Lat.	Long.	Component	PGA (Gal)	$R_{rup}$ (km)
San Juan	Capital	IDIA	− 31.53389	− 68.54385	E–W	166.77	86
					N–S	175.60	
San Juan	Capital	INPRES	− 31.52819	− 68.56121	E–W	189.51	87
					N–S	186.93	
					Vertical	150.46	
Mendoza	Capital	C de Ing	− 32.89018	− 68.84411	E–W	80.44	160
					N–S	84.37	
Mendoza	Rivadavia	El Carrizal Dam	− 32.92412	− 68.78272	E–W	81.24	200
					N–S	94.84	
					Vertical	19.20	

IDIA (San Juan): Instituto de Investigaciones Antisísmicas, Facultad de Ingeniería de la Universidad Nacional de San Juan, San Juan, Argentina

INPRES: Instituto Nacional de Prevención Sísmica, San Juan, Argentina

C de Ing.: Centro de Ingenieros building Mendoza, Argentina

**Table 2** Maximum accelerations (PGA) recorded during the 1985 ( $M_w$  5.9) Mendoza earthquake for eleven instruments showing their locations in the first three columns, component, Peak Ground Accelerations (PGA) values and distance to the epicenter  $R_{rup}$ 

Province	Locality	Site	Lat.	Long.	Component	PGA (Gal)	$R_{rup}$ (km)
Mendoza	Capital	AMICIS School	− 32.91782	− 68.83207	E–W	332.13	28
					N–S	272.26	
Mendoza	Capital	C de Ing	− 32.89018	− 68.84411	E–W	164.81	24
					N–S	79.53	
					Vertical	67.38	
Mendoza	Rivadavia	El Carrizal Dam	− 32.92412	− 68.78272	E–W	102.16	20
					N–S	111.15	
Mendoza	Lavalle	Municipality	− 32.88408	− 68.82107	E–W	62.98	48
					N–S	59.77	
Mendoza	Las Heras	Municipality	− 32.84922	− 68.81560	E–W	408.47	30
					N–S	191.90	
Mendoza	Maipu	Municipality	− 32.96725	− 68.78256	E–W	190.16	16
					N–S	58.24	
Mendoza	San Martin	Municipality	− 33.07991	− 68.46948	E–W	78.72	32
					N–S	79.73	
Mendoza	Tunuyán	Municipality	− 33.57011	− 69.01274	E–W	112.26	55
					N–S	115.68	
Mendoza	Uspallata	Gendarmería	− 32.58988	− 69.34559	E–W	114.83	77
					N–S	66.80	
Mendoza	Potrerillos	Potrerillos Hotel	− 32.95081	− 69.20567	E–W	109.55	40
Mendoza	Capital	Agua y Energía building	− 31.52819	− 68.84965	N–S	110.39	25
					Vertical	73.25	

C de Ing.: Centro de Ingenieros building Mendoza, Argentina

## 2 The last two large earthquakes in central-western Argentina

### 2.1 The 1977 ( $M_w$ 7.5) San Juan earthquake

The 1977 San Juan earthquake occurred on 23 November at 6 h 26 min local time with a centroid located at 31.220°S and 67.690°W. The moment magnitude obtained from modeling of teleseismic waveforms was  $M_w$  7.5 (Langer and Hartzell 1996) and the maximum Modified Mercalli intensities were  $I_{MM}$  IX to X (INPRES 1977). Seismic source studies indicate that this earthquake consisted of two sources located at middle crustal depths separated by approximately 60 km in horizontal distance and 20 s in origin time (Kadinsky-Cade et al. 1985). Their epicenters have been associated to a blind reverse-fault system beneath the Sierra Pie de Palo (PP) in the western Sierras Pampeanas (Fig. 1). According to Langer and Hartzell (1996) the first  $M_w$  7.1 event (Foreshock) was located at the northeast of this range and the second  $M_w$  7.4 event (Mainshock) at the southeastern flank of the Sierra Pie de Palo. For the purpose of energy release and distance calculations, we considered a magnitude  $M_w$  7.5 and the centroid of this earthquake located at 20.8 km depth provided by the Global Centroid Moment Tensor Project (Dziewonnski et al. 1981; Ekström et al. 2012). Because of this earthquake, 70 fatal

**Table 3** SA values registered during the 1977 ( $M_w$  7.5) San Juan earthquake. It is indicated the location of the instruments in the first three columns, then  $C_{SIS}$  denotes the seismic coefficient, SA the spectral acceleration and  $R_{rup}$  the distance to the epicenter as described in the text

Province	Locality	Site	Lat.	Long.	$C_{SIS}$	SA T=0.7 seg	Rrup (km)
Córdoba	Sampacho	Police station	- 33.38412	- 64.72278	0.10	98.0	359
Córdoba	Capital	Hospital Privado	- 31.39977	- 64.18333	0.09	88.2	343
Córdoba	Villa Dolores	Ex. Policlínico Ferroviario building	- 31.42281	- 64.18450	0.07	68.6	250
Córdoba	Río Cuarto	Municipality	- 33.10127	- 64.33426	0.07	68.6	377
Córdoba	Capital	Hospital Nacional Clínicas	- 31.40631	- 64.20401	0.06	58	343
Córdoba	Capital	Club Municipal	- 31.42062	- 64.18709	0.06	58.8	343
Córdoba	Cruz del Eje	Municipality	- 30.74444	- 64.79028	0.04	39.2	292
Córdoba	Capital	Obras Públicas building	- 31.40817	- 64.18831	0.04	39.2	343
Córdoba	Salsacate	Municipality	- 31.31794	- 65.08979	0.03	29.4	252
Córdoba	Carlos Paz	Municipality	- 31.41742	- 64.49427	0.03	29.4	310
La Rioja	Chamical	Municipality	- 29.41501	- 66.83418	0.24	235.2	179
La Rioja	Capital	Building	- 29.42970	- 66.86701	0.09	88.2	236
La Rioja	Chilecito	Municipality	- 29.16234	- 67.49932	0.05	49.0	250
La Rioja	Aimogasta	Municipality	- 28.55496	- 66.81729	0.04	39.2	326
San Juan	Caucete	IDIA station	- 31.65075	- 68.28150	0.55	539.0	64
San Juan	Caucete	Police station	- 31.65410	- 68.28528	0.55	539.0	64
San Juan	9 de Julio	Airport	- 31.57139	- 68.41846	0.48	470.4	75
San Juan	Media Agua	Police station	- 31.98268	- 68.41991	0.44	431.2	98
San Juan	Capital	Vialidad Nacional	- 31.52564	- 68.51569	0.42	411.6	81
San Juan	Albardón	Municipality	- 31.43902	- 68.52099	0.37	362.6	80
San Juan	Capital	G. Rawson School	- 31.52234	- 68.52326	0.37	362.6	82
San Juan	Capital	Hospital Español	- 31.55208	- 68.53428	0.35	343.0	86
San Juan	Capital	J. Fontana School	- 31.53426	- 68.55890	0.34	333.2	84
San Juan	Capital	9 de Julio Building	- 31.53915	- 68.51618	0.30	294.0	82

**Table 3** (continued)

Province	Locality	Site	Lat.	Long.	C <sub>sis</sub>	SA T=0.7 seg	Rrup (km)
San Juan	Rinconada	IDJA station	- 31.69271	- 68.58767	0.30	294.0	96
San Juan	Rivadavia	P. de Mendoza School	- 31.56025	- 68.54963	0.26	254.8	87
San Juan	Capital	IDJA station	- 31.53389	- 68.54385	0.26	254.8	86
San Juan	Santa Lucía	Nacional N° 2 School	- 31.53025	- 68.50526	0.26	254.8	81
San Juan	Santa Lucía	Pellegrini School	- 31.55022	- 68.47647	0.24	235.2	80
San Juan	Capital	INPRES	- 31.52819	- 68.56121	0.23	225.4	88
San Juan	Capital	INPRES	- 31.52819	- 68.56121	0.22	215.6	88
San Juan	Calingasta	El Tambolar	- 31.18330	- 68.88330	0.11	107.8	133
San Juan	Calingasta	Police station	- 31.33294	- 69.41726	0.11	107.8	172
San Juan	Jachal	Fire station	- 30.24237	- 68.74638	0.08	73.5	168
San Juan	Barreal	Gendarmería	- 31.68636	- 69.49524	0.06	58.8	180
San Juan	Ullum	San Juan River	- 31.47776	- 68.64936	0.05	49.0	115
San Juan	Pismanta	Pismanta hotel	- 30.27887	- 69.22901	0.05	49.0	196
San Luis	Capital	Policlínico Ferroviario	- 33.29913	- 66.34813	0.07	72.5	252
San Luis	Villa Mercedes	Municipality	- 33.67453	- 65.46195	0.07	71.5	336

**Table 4** SA values registered during the 1985 ( $M_w$  5.9) Mendoza earthquake. It is indicated the location of the instruments in the first three columns, then  $C_{SI}$  denotes the seismic coefficient, SA the spectral acceleration and  $R_{rup}$  the distance to the epicenter as described in the text

Province	Locality	Site	Lat.	Long.	$C_{SI}$	SA ( $T=0.7$ s) 10%	$R_{rup}$ (km)
Mendoza	Godoy Cruz	Municipality	− 32.91782	− 68.83207	0.37	362.6	22
Mendoza	Capital	Architecture Faculty	− 32.89018	− 68.84411	0.21	205.8	26
Mendoza	Las Heras	Municipality	− 32.84922	− 68.81560	0.27	264.6	30
Mendoza	Maipú	Municipality	− 32.96725	− 68.78256	0.2	196	15
Mendoza	Lavalle	Municipality	− 32.88408	− 68.82107	0.067	65.66	49
Mendoza	San Martín	Municipality	− 33.07991	− 68.46948	0.062	60.76	32
Mendoza	Potrerillos	Potrerillos Hotel	− 32.95081	− 69.20567	0.051	49.98	40
Mendoza	Capital	Sismological Station	− 32.89018	− 68.84411	0.28	274.4	26
Mendoza	Capital	Facultad Regional UTN	− 32.89702	− 68.85314	0.18	176.4	25
Mendoza	Capital	Galería Tonsa	− 32.89008	− 68.83710	0.16	156.8	26
Mendoza	Capital	Municipality	− 32.89808	− 68.84331	0.11	107.8	25
Mendoza	Capital	Municipality	− 32.89808	− 68.84331	0.33	323.4	25
Mendoza	Capital	Municipality	− 32.89808	− 68.84331	0.48	470.4	25
Mendoza	Capital	Government House	− 32.89828	− 68.84628	0.026	25.48	25
Mendoza	Rivadavia	El Carrizal Dam	− 33.29321	− 68.73158	0.13	127.4	20
Mendoza	Uspallata	Gendarmeria	− 32.59110	− 69.34789	0.08	78.4	77
Mendoza	Capital	San Antonio Mono- block	− 32.87257	− 68.83092	0.044	43.12	28
Mendoza	Tunuyan	Municipality	− 33.58125	− 69.01530	0.08	78.4	55

victims and around 209 seriously injured people were reported in the province of San Juan (INPRES 1977).

The greatest damage and number of victims occurred in the city of Caucete, which is located 30 km to the southeast of downtown San Juan (Fig. 1). In addition, minor damage was reported for some buildings in Córdoba, 400 km to the east of the epicenter. The vibrations were also felt in Buenos Aires, Santiago (Chile), Montevideo (Uruguay), Asunción (Paraguay) and even in the high buildings of Porto Alegre and Sao Pablo (Brazil) as far as 1500 km away. Collapses and serious structural damage occurred in adobe constructions without reinforcements (INPRES 1977). Liquefaction effects were quantified in an area of around 1000 km<sup>2</sup> causing damage to vineyards, irrigation canals, routes and railroads. Figure 3 shows the derailment of a freight train that was circulating at a low speed during the 1977 earthquake near Caucete, due to the strong motion produced by near-field seismic waves.

## 2.2 The 1985 ( $M_w$ 5.9) Mendoza earthquake

On Saturday 26 January 1985 at 00 h 07 min local time, a seismic event occurred in Mendoza with a magnitude  $M_w$  5.9 and maximum intensities  $I_{MM}$  VII to VIII (INPRES 1986). The centroid location provided by the Global Centroid Moment Tensor Project (Dziwonski et al. 1981; Ekström et al. 2012) indicated 33.11°S and 68.75°W and 28.4 km





**Fig. 3** Derailment of a freight train at approximately 31.5°S and 67.6°W that was traveling at a low speed due to the strong motion of the ( $M_w$  7.5) San Juan earthquake on 23 November 1977 (Photograph courtesy of the Instituto de Investigaciones Antisísmicas—UNSJ 1977)

depth. Local studies determined the hypocenter at 33.12°S and 68.82°W, 12 km depth, on a blind thrust fault associated to the Barrancas anticline in the southwest of Mendoza city (Chiaramonte et al. 2000). In Godoy Cruz, at an approximately epicentral distance of 37 km, the locality of Villa Hipódromo (32.91°S, 68.83°W) recorded the total collapse of the old Hospital del Carmen. Although its moderate magnitude  $M_w$  5.9, this earthquake caused the death to 6 people, injures to 238 people and severe damage to more than 12,000 houses, which were mainly built of adobe (Fig. 4). Overall, the cities of Mendoza and Las Heras were more affected, as well as those areas located in paleochannels (INPRES 1986). This earthquake in 1985, however, is not considered the most damaging in history. In fact, a previous earthquake on 20 March 1861 devastated almost the entire city of Mendoza leaving in ruins the Foundational San Francisco area located at an approximately epicentral distance of 15 km. The number of deaths was about 6000 to 8000 over a population of 13,000 to 18,000 as reported by INPRES (1986).

### 3 Data and methods

Peak ground acceleration (PGA) data were obtained from analog strong-motion AR-240, Ishimoto and SMA-1 photographic tri-axial accelerographs with maximum acceleration record of 1 g. Four observations were acquired for the 1977 earthquake (Fig. 2 and Table 1). The network was expanded by the time of the 1985 earthquake occurrence providing 11 PGA observations (Fig. 2 and Table 2). The data from the film were converted to paper copies and then, recovered by manual digitalization to obtain ASCII files. Figure 5 shows the more than one-minute horizontal E-W component acceleration record of the



**Fig. 4** Totally collapsed houses after the Mendoza ( $M_w$  5.9) earthquake on 26 January 1985 (Diario Los Andes, Mendoza, Argentina in the 2016 earthquake anniversary edition)

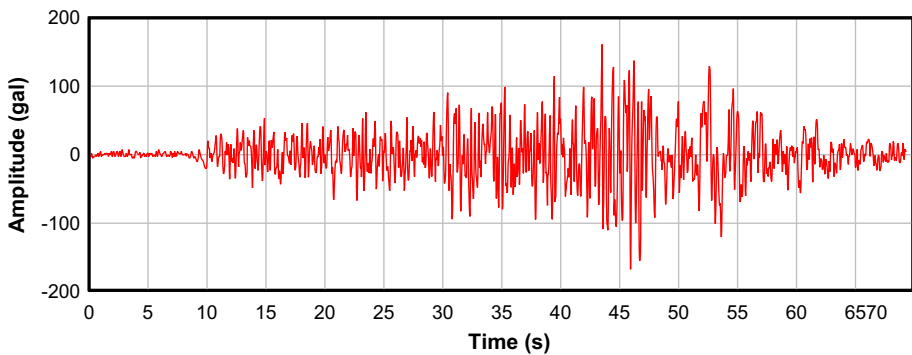


**Fig. 5** Accelerogram of the 1977 ( $M_w$  7.5) San Juan earthquake recorded at 86 km epicentral distance at the building of the Instituto de Investigaciones Antisísmicas of the Universidad Nacional de San Juan, San Juan Argentina

1977 San Juan earthquake. Maximum amplitude of 166.8 Gal was observed for the E–W component at a distance of 86 km to the southwest of the epicenter.

Figure 6 shows the E–W horizontal component of one accelerogram of the 1985 Mendoza earthquake. This record with duration of about 5 s was obtained in Las Heras at a distance of 30 km north of the epicenter. The maximum recorded acceleration was 408 Gal (E–W component), which was greater than that in the N–S component (192 Gal) at the same location. PGA values were considered for the closest site-to-rupture distance ( $R_{rup}$ ) in order to compare them to global empirical databases.

Spectral Acceleration (SA) data were obtained from Wilmot-type seismoscopes (Hudson 1958; Cloud and Hudson 1961). This instrument is a damped two-degree-of-freedom oscillator capable of recording the pendulum trajectory in a horizontal plane. Using a needle on a smoked glass, this instrument traces a hodogram representing the response

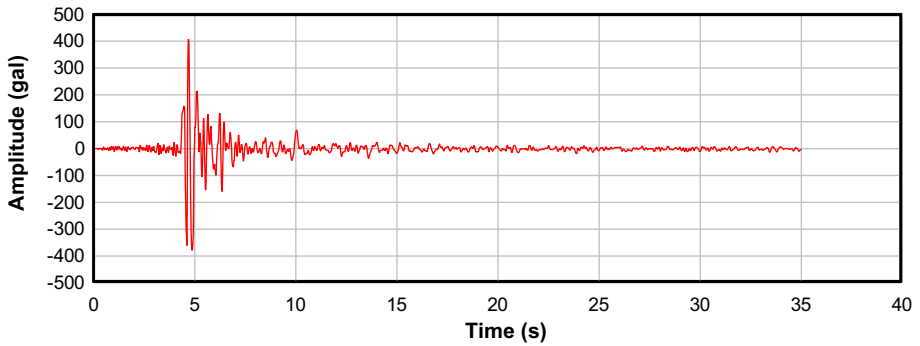


**Fig. 6** E-W component accelerogram for the 1985 ( $M_w$  5.9) Mendoza earthquake recorded at the Municipality of Las Heras (Mendoza) at an epicentral distance of 30 km

of a lightly damped pendulum to the earthquake excitation (Lomnitz 2012). The resulting record indicates the direction and amplitude of the horizontal motion, but without time record (Fig. 7).

Using the smoked plates it was possible to estimate the  $C_{sis}$  parameter as stated in the equation  $C_{sis} = \tan(S \cdot d)$ , where  $S$  is the sensitivity in rad/mm usually provided by the manufacturer (e.g. mean value of  $S=0.023$  rad/mm, approximately); and  $d$  is the maximum distance in millimeter to the center of the glass record. These  $C_{sis}$  values obtained from the seismoscopes can be correlated with the building dynamic parameters. Using the

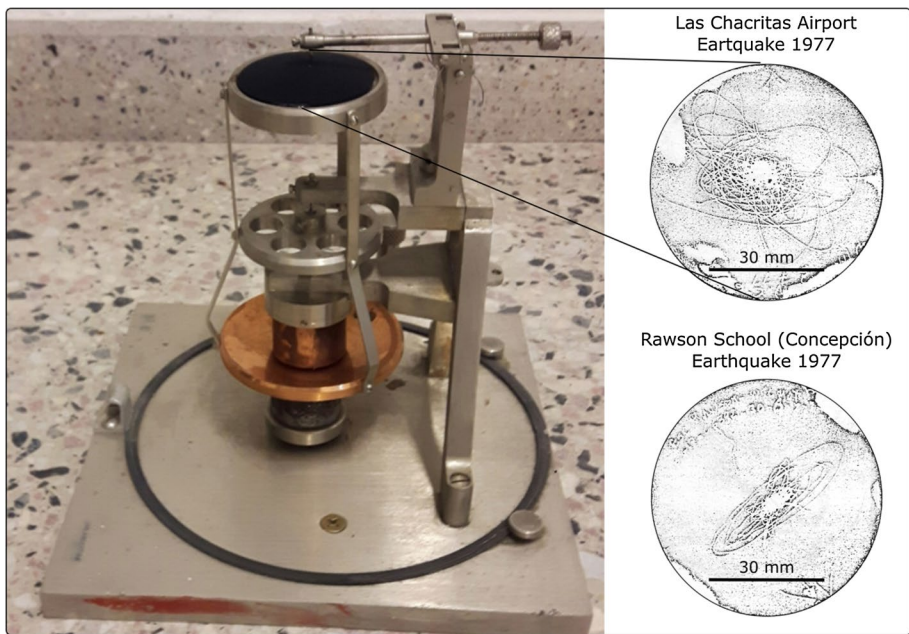


**Fig. 7** Wilmot-type seismoscope and two records obtained during the 1977 ( $M_w$  7.5) San Juan earthquake (see locations in Table 3 and Fig. 2)

$C_{\text{sis}}$  database, we calculated the spectral accelerations SA corresponding to 0.7 s period and 10% damping. This was done using the equation  $SA = C_{\text{sis}} \cdot g$ , where  $g$  is the gravity average value (980 Gal). As a result, 39 SA values were calculated for the 1977 San Juan earthquake (Fig. 2 and Table 3) and 18 SA values for the 1985 Mendoza earthquake (Fig. 2 and Table 4).

Due to the lack of information, PGA and SA data were not corrected for source directivity and topographic amplification as suggested by other authors (e.g., Harmsen 1997; Somerville et al. 1997).

### 3.1 Empirical response spectral attenuation relations

Empirical response spectral attenuation relationships relate magnitude, distance and macroseismic intensity data to predict the accelerations caused by a seismic event. Less damage of an earthquake is expected as the distance from the rupture area increases. This is due to the seismic wave propagation in the crust, including geometrical spreading (a decrease in amplitude of the waves with distance at successive wavefronts) as well as anelastic and scattering attenuation.

Abrahamson and Silva (1997) have proposed a spectral acceleration attenuation relationship based on distance and magnitude for different structural periods, using shallow earthquakes of magnitudes greater than  $M_w$  4.4. Thus, a set of curves characterize different tectonically active regions worldwide and different types of faults. Sadigh et al. (1997) have developed attenuation relationships for peak accelerations and response spectral accelerations for crustal earthquakes of magnitudes greater than 4 in the western United States. In both cases, rock and soil site conditions were considered. In addition, Abrahamson and Silva (2008) obtained curves valid for earthquakes ranging from  $M_w$  5 to 8.5 and for spectral periods of 0 to 10 s. In these curves, the site category is parameterized by average shear wave velocities at 30 m and 1000 m depths corresponding to models Vs30 and Vs1000, respectively.

In this study, measured PGA values were compared with mean theoretical values predicted by Abrahamson and Silva (1997, 2008) and Sadigh et al. (1997). Similarly, SA values were compared to those by Abrahamson and Silva (1997) for a period of 0.7 s and a 10% damping in soil and rock.

### 3.2 Surface wave radiation pattern

Due to the shear failure mechanisms of earthquakes, amplitudes of seismic waves vary with the azimuth from the epicenter and the wavenumber (Rösler and van der Lee 2020). In this context, the surface-wave radiation pattern determines the azimuthal variation of the amplitude and sense of motion of the wavefronts near the source (Lay and Wallace 1995). It depends on the source process, the depth and the frequency of the seismic waves (IRIS DMC 2020). Basically, the radiation pattern shows spectral amplitudes in [m/Hz], which have been calculated assuming a continental lithosphere model (e.g. the iasp91 Earth model) for Rayleigh and Love waves (Rösler and van der Lee 2020). In this work, the surface-wave radiation patterns were calculated considering the geometry of the faults; this information is obtained from data in the CMT World Catalog (Dziewonski et al. 1981; Ekström et al. 2012) for events in 1977 and 1985. The assumed geometry of the fault and depth of the source for the 1977 San Juan earthquake are a strike = 4°, dip = 46°, slip = 90°

and focal depth=20.8 km; while for the 1985 Mendoza earthquake are strike=5°, dip=37°, slip=80° and focal depth= 12 km.

## 4 Results and discussion

### 4.1 Maximum accelerations recorded during the 1977 ( $M_w$ 7.5) San Juan earthquake

Four PGA measurements for the 1977 San Juan earthquake were obtained at  $R_{rup}$  distances of 60 to 80 km and 160 to 200 km, showing maximum values of 166 Gal and 85 Gal, respectively for the horizontal components. These values were compared to those predicted by Abrahamson and Silva (1997, 2008) and Sadigh et al. (1997) for a similar seismic source of magnitude  $M_w$  7.5 and a reverse faulting mechanism. For  $R_{rup}$  distances of 60 to 80 km, PGA values are 100 Gal above the Abrahamson and Silva (1997) predictions for soil and rock and 130 Gal above the Abrahamson and Silva (2008) values for rock predictions. For  $R_{rup}$  distances of about 180 km, these differences are between 30 and 60 Gal above the Abrahamson and Silva (1997) and 55 to 75 Gal above the Abrahamson and Silva (2008) predictions (Fig. 8). This evaluation indicates that the approximation gets better

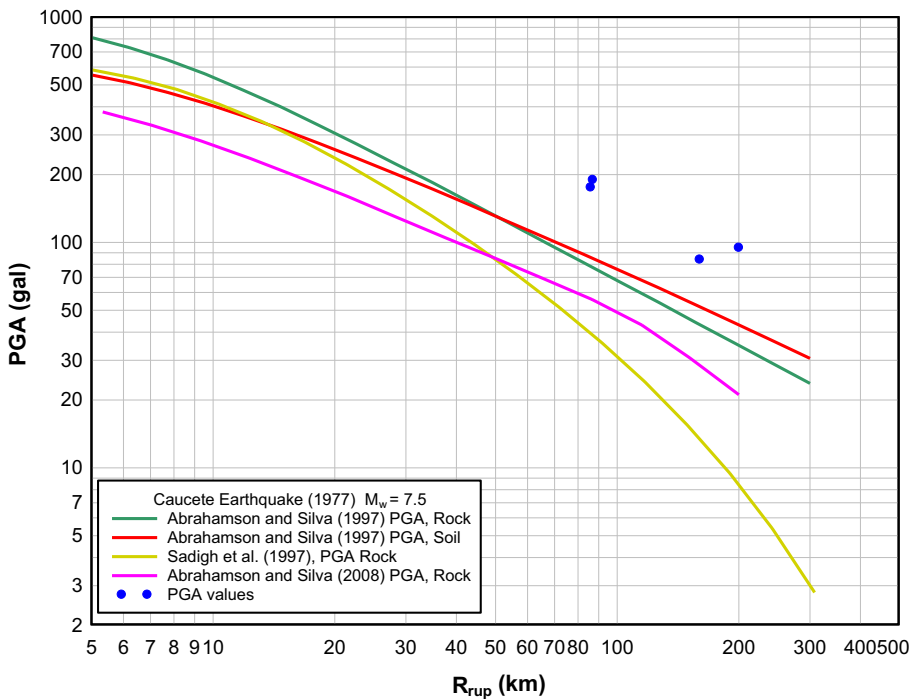


**Fig. 8** Comparison of PGA data for the 1977 San Juan ( $M_w$  7.5) earthquake with PGA attenuation curves determined by different global studies for shallow earthquakes as a function of the  $R_{rup}$  distance. The predicted curves assume a similar  $M_w$  7.5 seismic source magnitude and a reverse faulting mechanism

when comparing our values with those from the Abrahamson and Silva (1997) curve for soil and rock.

The comparison using the Abrahamson and Silva (2008) curve produces greater differences in PGA values at any  $R_{rup}$  distance. It is worth to note that the average Abrahamson and Silva (1997) attenuation curve assumes a  $Vs30$  of 550 m/s while the Abrahamson and Silva (2008) curve considers a  $Vs30$  of 760 m/s. Thus, an optimal attenuation curve able to predict our PGA observations should involve smaller than 550 m/s  $Vs30$  values. A final comparison of our PGA values to those predicted by Sadigh et al. (1997) for rock produces higher differences.

Because the PGA results are better predicted by the attenuation curves from Abrahamson and Silva (1997) for soil and rock, we decided to use the same database for a similar comparison between SA values. In this case, a structural period of 0.7 s and a damping of 10% were considered. Figure 9 shows the SA values estimated from records of seismoscopes as a function of the  $R_{rup}$  distance. Superimposed are the corresponding predicted SA curves by Abrahamson and Silva (1997). SA observations can be separated in two groups G1 and G2. Group G1 represents data at  $R_{rup}$  distances between 60 and 100 km and SA values between 220 and 550 Gal; these values are above those predicted by the average attenuation curves by Abrahamson and Silva (1997). Differences in SA values among 100 and 400 Gal are observed for rock conditions while smaller differences of 50 to 350 Gal are obtained for soil conditions. Group G2 represents data at  $R_{rup}$  distances between 150 and

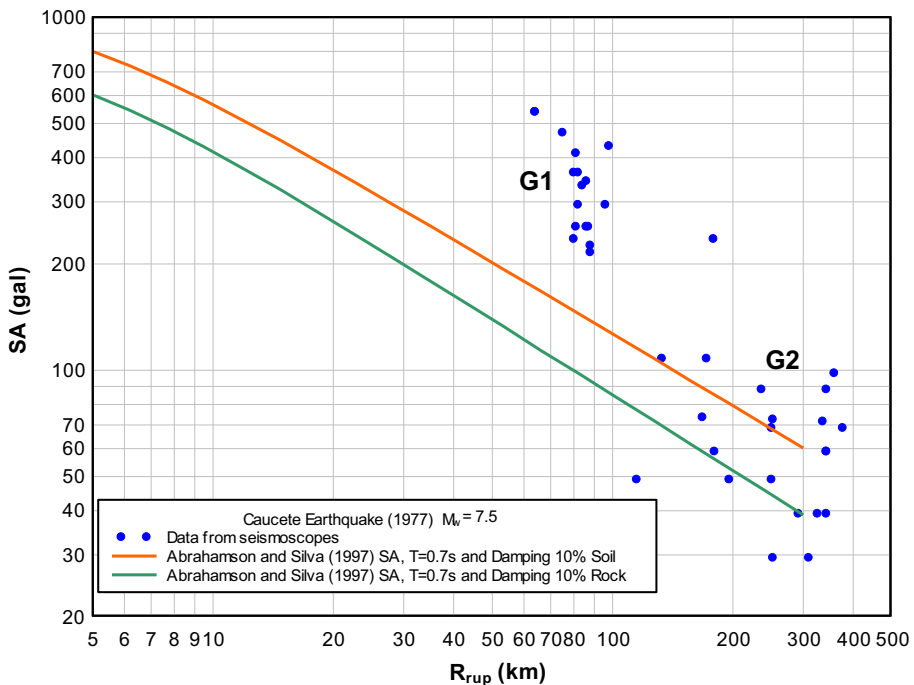


**Fig. 9** Comparison between the attenuation curves from Abrahamson and Silva (1997) as a function of the  $R_{rup}$  distance (for crustal earthquakes) with the SA maximum horizontal component values observed for a structural period of 0.7 s and a 10% damping during the 1977 San Juan ( $M_w$  7.5) earthquake. Data in Groups G1 and G2 are discussed in the text

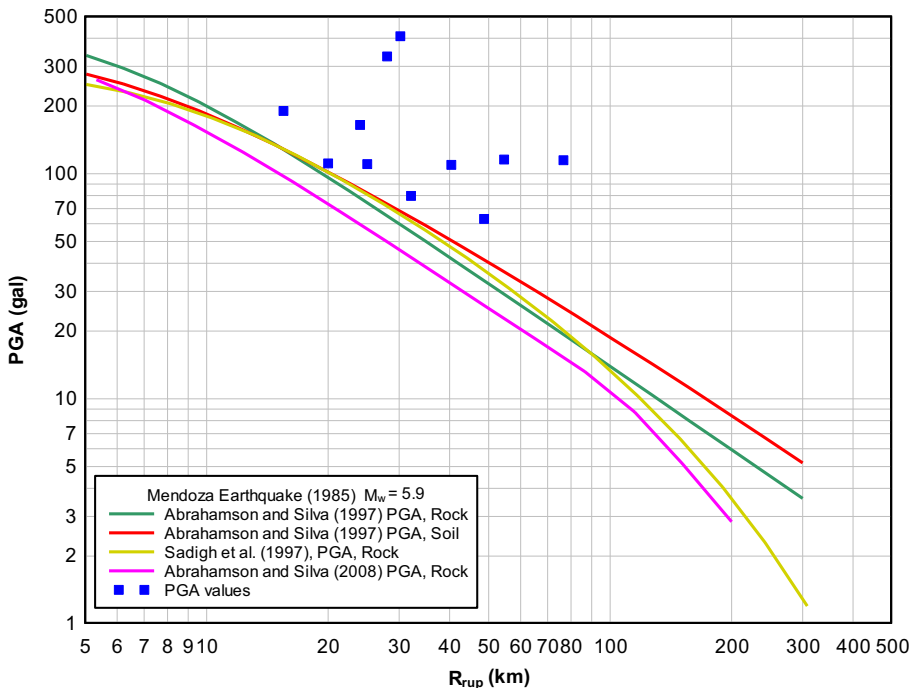
380 km. Although the SA values for this group (G2) show some dispersion, both Abrahamson and Silva (1997) average attenuation curves for soil and rock produce a better fit to the SA observations in comparison to those of Group G1.

Our results suggest that the amplification in the SA values at  $R_{rup}$  distances of less than 100 km (group G1) could be explained due to the presence of site effects. The observed SA values at longer  $R_{rup}$  distances (group G2) are consistent with the predicted values by Abrahamson and Silva (1997) using a  $Vs30$  of 550 m/s.

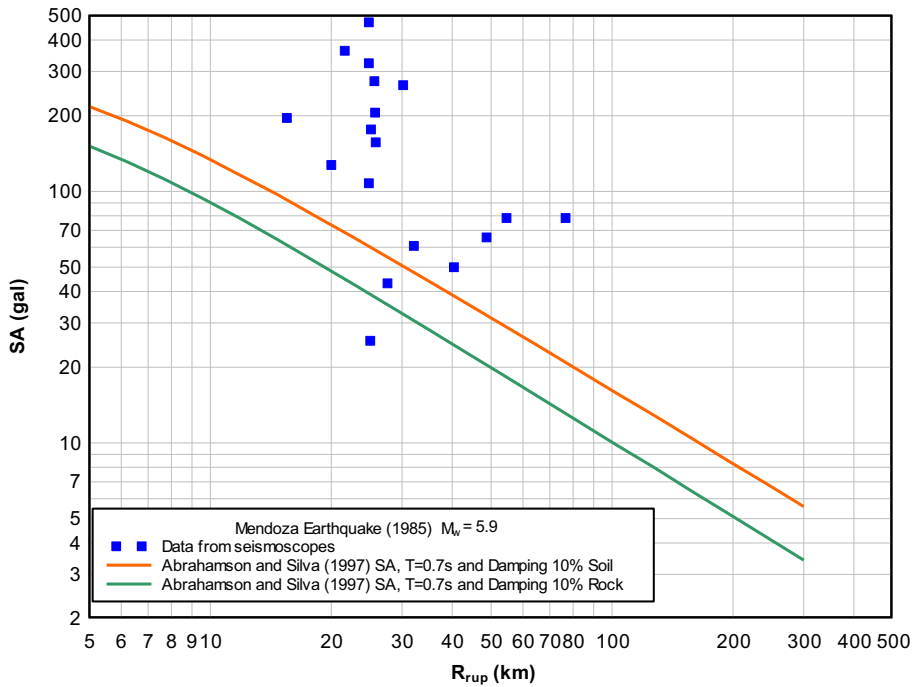
### 4.2 Maximum accelerations recorded during the 1985 ( $M_w$ 5.9) Mendoza earthquake

Figure 10 shows 11 PGA values between 60 and 408 Gal for the 1985 Mendoza earthquake as a function of  $R_{rup}$  distances of 18 to 80 km. Superimposed in the same figure are the attenuation curves of Abrahamson and Silva (1997, 2008) and Sadigh et al. (1997) assuming a same sized magnitude and a reverse fault seismic source.

Most of the PGA values are above those predicted by the attenuation curves. In particular, observations at  $R_{rup}$  distances of 28 and 30 km show exceptional high values of 332 and 408 Gal, respectively. The attenuation curves are located approximately 350 Gal below the observed PGA values for the same distances. These locations correspond to the localities Maipú (10 km to the southeast of Mendoza city) and Las Heras (5 km to the north



**Fig. 10** Maximum PGA values recorded for the horizontal components during the 1985 Mendoza ( $M_w$  5.9) earthquake as a function of  $R_{rup}$  distance. Also shown, is a comparison between these values with global average attenuation estimations for crustal earthquakes. The predicted curves were generated for a  $M_w$  5.9 magnitude and a reverse fault seismic source



**Fig. 11** Comparison between SA attenuation curves from Abrahamson and Silva (1997) as a function of  $R_{rup}$  distance (for shallow earthquakes) with the maximum horizontal component values calculated for a structural period of 0.7 s and a 10% damping during the 1985 ( $M_w$  5.9) Mendoza earthquake

of downtown Mendoza) evidencing a significant amplification of the ground acceleration. Overall, the Abrahamson and Silva (1997) curve for soil conditions shows a better approximation to the observations.

18 SA observations for the 1985 Mendoza earthquake are shown in Fig. 11. These values were obtained from seismoscopes at  $R_{rup}$  distances between 15 and 77 km and compared to the global attenuation curves. 16 SA values lie above the predictions from Abrahamson and Silva (1997) for soil and only two values are below this curve. For  $R_{rup}$  distances between 20 and 30 km, SA values vary between 110 and 450 Gal; the predicted values in the same distance range indicate lower values of 50 to 70 Gal.

PGA and SA values for the 1977 and 1985 earthquakes, which were caused by similar blind reverse-fault activity, indicate higher values than those predicted by global attenuation empirical relationships. The 1985 Mendoza earthquake produced very high ground accelerations although it had a moderate magnitude  $M_w$  5.9. This event occurred beneath the most populated area of Mendoza and was associated to a shallow depth seismic source of about 12 km.

### 4.3 Regional-scale $V_{s30}$ information and surface wave energy radiation

The acceleration amplifications with respect to the mean theoretical values as a function of the azimuth to each seismic event were evaluated. The available information was integrated with data from the United States Geological Service  $V_{s30}$  Global Server (<https://>



[earthquake.usgs.gov/vs30/](https://earthquake.usgs.gov/vs30/)). Several studies have discussed the advantages and disadvantages of using the average shear wave velocities at 30 m depth ( $V_{s30}$ ) for evaluating global seismic site conditions (e.g., Castellaro et al. 2008; Allen and Wall 2009; Sairam et al. 2011). Moreover, these data were compared with the theoretical values of the surface wave radiation patterns for both earthquakes generated using the IRIS Data Services (IRIS DMC 2020).

For the 1977 San Juan earthquake, only four maximum horizontal PGA values are available at two  $R_{rup}$  distances of approximately 60 km and 200 km with azimuths ranging from  $220^\circ$  to  $270^\circ$  (Figs. 2, 8, 12). While this amount of data is very limited with respect to the azimuthal coverage, an amplification of up to 150 Gal can be noted for this range. Furthermore, the values obtained in areas with low  $V_{s30}$  are the most amplified. On the other hand, the distribution of SA for the 1977 earthquake almost completely covers the full range of azimuths at  $R_{rup}$  distances from 60 to 400 km (Figs. 2, 9, 12). In this case, a preferential direction of  $240^\circ$  in the amplifications (values up to 400 Gal) is observed for stations in low  $V_{s30}$  zones. In contrast, accelerations at those stations located in areas of high  $V_{s30}$  were not significantly amplified. Overall, the maximum amplification directions are consistent with the diagrams of surface-wave radiation pattern, especially for Love waves.

During the 1985 ( $M_w$  5.9) Mendoza earthquake, 11 PGA values were measured at  $R_{rup}$  distances between 15 and 80 km covering much of the azimuthal range (Figs. 2, 10, 13). These values show acceleration amplifications of up to 350 Gal for an azimuth of  $330^\circ$ . The observations of SA for the same earthquake also show a preferential amplification towards  $330^\circ$  (Fig. 13), but with higher values that reached 450 Gal. As in the case of the 1977 San Juan earthquake, both graphs show that the greatest amplifications were produced in areas of low  $V_{s30}$ .

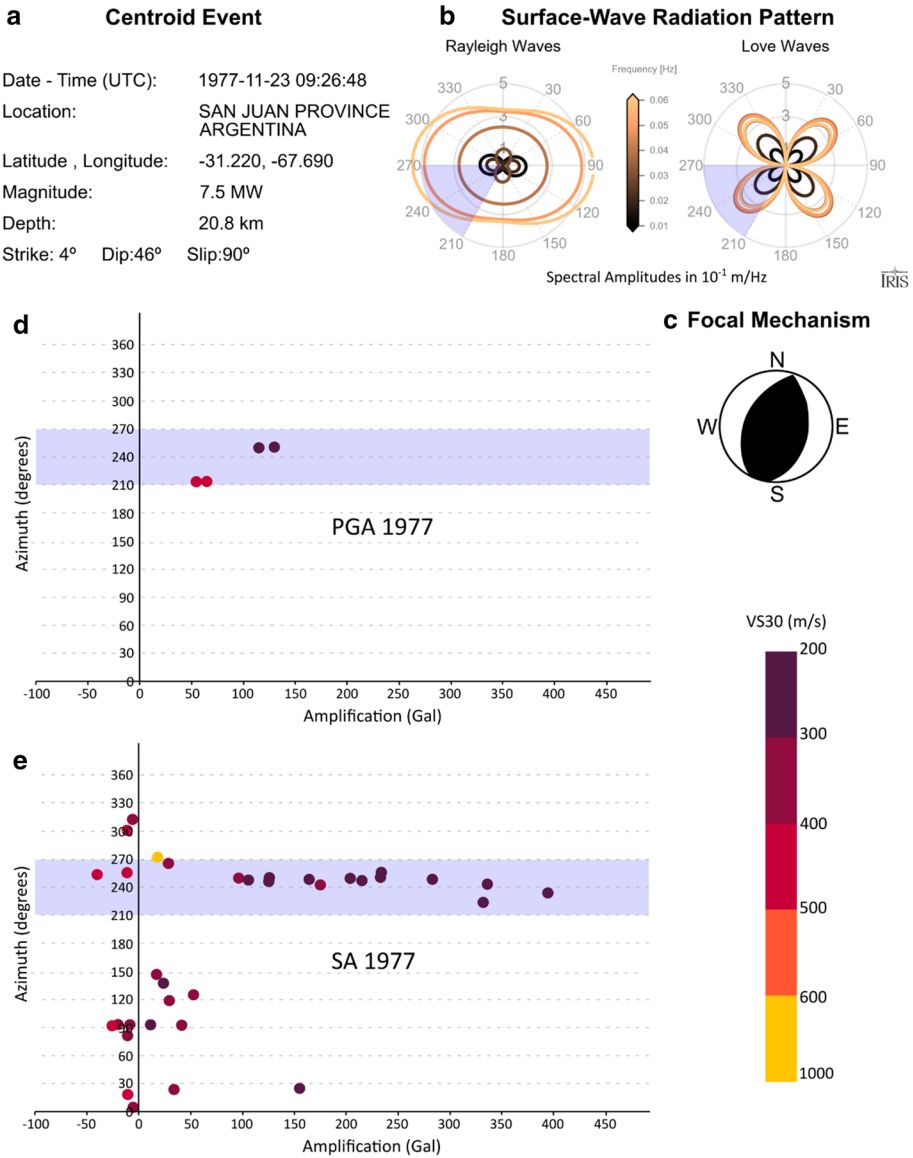
The analyzed data from the 1985 Mendoza earthquake (Fig. 13) revealed that the greatest amplifications in the ground accelerations (values up to 450 Gal) occurred to the NNW of the epicenter and mainly in areas of low  $V_{s30}$ . The maximum amplification direction coincides with the NW quadrant of the surface wave radiation pattern diagram for love waves.

Figure 14 shows the direction of maximum amplification of the seismic waves superimposed on a map of  $V_{s30}$ . The red star for the 1977 San Juan earthquake represents the mean distance between the foreshock and the mainshock. As presented on the map, the cities of San Juan and Mendoza are located in areas of low  $V_{s30}$ , with values of 287 m/s and 368 m/s, respectively. This suggests that during an earthquake, populated areas in the near source areas would be under acceleration amplifications regardless of the direction of maximum earthquake energy radiation.

Given the small amount of data available for both historical earthquakes, it is very difficult to precisely attribute the amplification of the ground accelerations to site effects or the direction of maximum energy radiation of the earthquakes. Nevertheless, both factors contribute to the total acceleration values measured with accelerometers and seismoscopes.

## 5 Conclusions

We provide evidence that site amplification effects are present in the measured ground accelerations caused by moderate-to-large earthquakes during 1977 and 1985 in western central Argentina and should be considered in seismic hazard analyses. However, these effects can be enhanced by directionality of maximum wave radiation. The comparison of



**Fig. 12** Analysis of the 1977 San Juan earthquake data. **a** Centroid data from the Global CMT Project and Langer and Hartzell (1996). **b** Surface wave radiation pattern obtained from IRIS DMC (2020). **c** Focal mechanism obtained from the Global CMT Project. **d** PGA amplifications and Vs30 velocities vs. azimuth from the epicenter of the seismic event. **e** SA amplifications and Vs30 velocities vs. azimuth from the epicenter of the seismic event

the data acquired during the 1977 ( $M_w$  7.5) San Juan earthquake with the global attenuation curves, shows that ground acceleration amplifications of up to 394 Gal is consistent with a preferential azimuth of 240°, mainly towards the cities of San Juan and Caucete. The measured acceleration value of 539 Gal represents an increase of 270% with respect

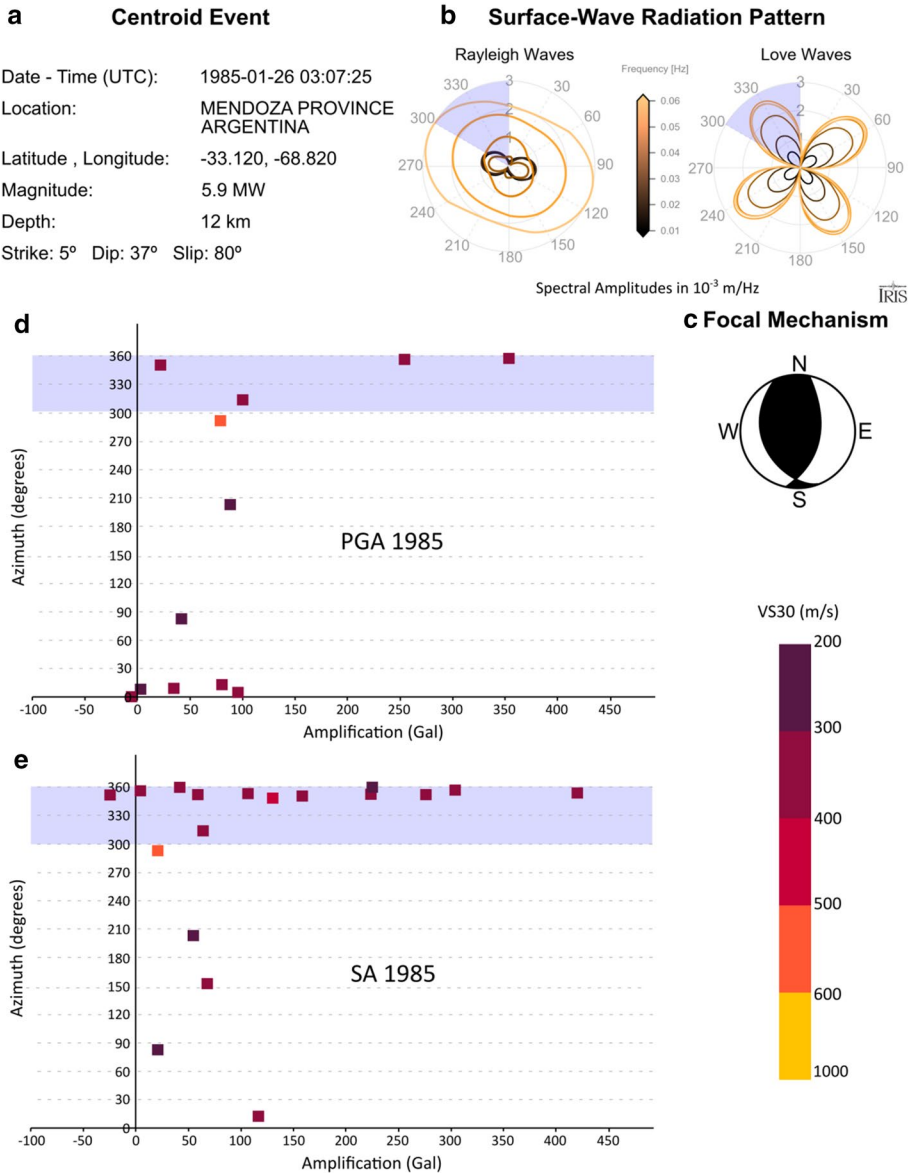


**Fig. 13** Analysis of the 1985 Mendoza earthquake data. **a** Centroid data from the Global CMT Project. **b** Surface wave radiation pattern obtained from IRIS DMC (2020). **c** Focal mechanism obtained from the Global CMT Project. **d** PGA amplifications and Vs30 velocities versus azimuth from the epicenter of the seismic event. **e** SA amplifications and Vs30 velocities versus azimuth from the epicenter of the seismic event

to the expected theoretical acceleration of 145 Gal generated by an earthquake of similar characteristics.

The 1985 ( $M_w$  5.9) Mendoza earthquake generated ground acceleration amplifications with a preferential azimuth of  $330^\circ$  towards the city of Mendoza and the surrounding area.

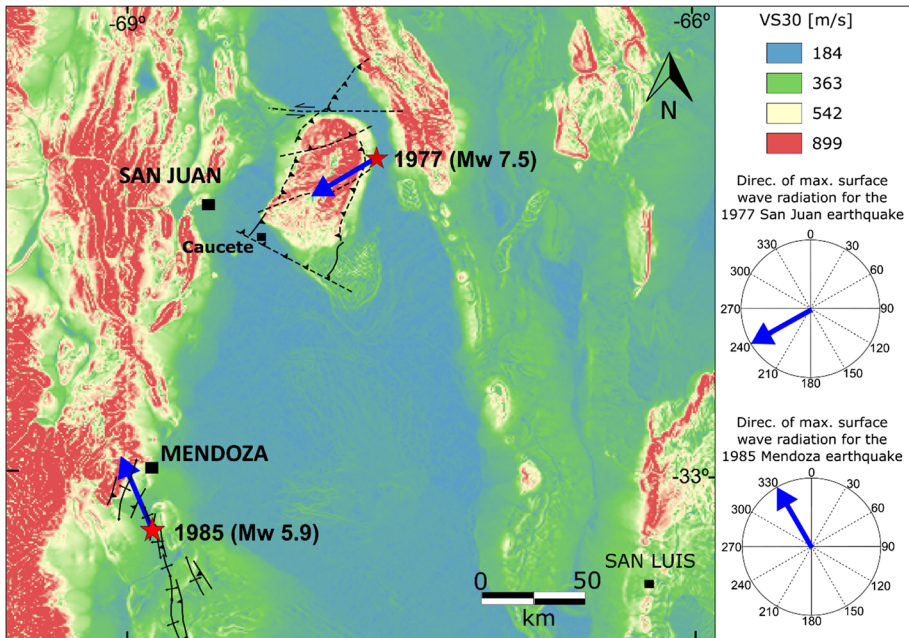


**Fig. 14** Vs30 map for the study area. Red stars indicate the epicenters of the 1977 San Juan and 1985 Mendoza earthquakes and blue arrows show the directions of maximum surface wave radiation

In this region, an amplification of 420 Gal was recorded. The measured value of 470 Gal is 840% higher than the 50 Gal expected in the area for a similar theoretical earthquake. This explains why a moderate magnitude earthquake produced ground accelerations with capability of damage of entire buildings.

Although site amplification effects are complex, it can be observed that these occur in areas of low Vs30 and with a preferential orientation of surface wave radiation pattern. In contrast, regions with high Vs30 values did not record large amplifications. Future large crustal earthquakes will probably have more detailed observations like horizontal and vertical accelerometer data, which are desirable in site amplification studies.

**Acknowledgements** We are particularly grateful to the USGS for providing access to the Global Vs30 Server (2020) for academic purposes. The authors would also like to acknowledge Consejo Nacional de Investigaciones Científicas y Técnicas (CONICET) for their research grants.

## References

- Abrahamson N, Silva W (1997) Empirical response spectral attenuation, relations for shallow crustal earthquakes. *Seismol Res Lett* 68(1):94–116
- Abrahamson NA, Silva W (2008) Summary of the Abrahamson and Silva NGA ground-motion relations. *Earthq Spectra* 24:67–97
- Allen TI, Wald DJ (2009) On the use of high-resolution topographic data as a proxy for seismic site conditions (VS30). *Bull Seism Soc Am* 99(2A):935–943
- Alvarado P, Beck S (2006) Source characterization of the San Juan (Argentina) crustal earthquakes of 15 January 1944 (Mw 7.0) and 11 June 1952 (Mw 6.8). *Earth Planet Sci Lett* 243(3–4):615–631

- Alvarado P, Araujo M (2011) La importancia de las redes sísmicas locales en la caracterización de la sismicidad cortical más peligrosa de la Argentina. In: Internacional conference in Honour of Ing. Alberto Giesecke M. Lima, Perú, pp 57–72
- Castellaro S, Mulargia F, Rossi PL (2008) VS30: Proxy for seismic amplification? *Seismol Res Lett* 79(4):540–543
- Chiaromonte L, Ramos VA, Araujo M (2000) Estructura y sismotectónica del anticlinal Barrancas, cuenca Cuyana, provincia de Mendoza. *Revista de la Asociación Geológica Argentina* 55(4):309–336
- Cloud WK, Hudson DE (1961) A simplified instrument for recording strong motion earthquakes. *Bull Seismol Soc Am* 51(2):159–174
- Dziewonski AM, Chou T-A, Woodhouse JH (1981) Determination of earthquake source parameters from waveform data for studies of global and regional seismicity. *J Geophys Res* 86:2825–2852. <https://doi.org/10.1029/JB086iB04p02825>
- Ekström G, Nettles M, Dziewonski AM (2012) The global CMT project 2004–2010: centroid-moment tensors for 13,017 earthquakes. *Phys Earth Planet Inter* 200–201:1–9. <https://doi.org/10.1016/j.pepi.2012.04.002>
- Gregori SD, Christiansen R (2018) Seismic hazard analysis for central-western Argentina. *Geod Geodyn* 9(1):25–33
- Gregori SD (1993) Estudio de riesgo sísmico en la República Argentina. Centro IITEP (Rusia) y MAFRE (España), Inedit. <https://www.cridlac.org/digitalizacion/pdf/spa/doc4354/doc4354.htm>
- Harmsen SC (1997) Determination of site amplification in the Los Angeles urban area from inversion of strong-motion records. *Bull Seismol Soc Am* 87(4):866–887
- Hudson DE (1958) The Wilnot survey type strong-motion earthquake recorder. In: *Earthquake Engineering Research Laboratory, California Institute of Technology Pasadena*
- INPRES (1977) El terremoto de San Juan del 23 de noviembre de 1977. Preliminar inform. San Juan
- INPRES (1986) Gran Mendoza, el núcleo urbano expuesto al mayor nivel de riesgo sísmico en la República Argentina. *Publicación Técnica N°10*. INPRES
- IRIS DMC (2020) Data services products: the surface-wave radiation patterns. <https://doi.org/10.17611/DP/SWRP.1>
- Kadinsky-Cade K, Reilinger R, Isacks B (1985) Surface deformation associated with the November 23, 1977, Cauçete, Argentina, earthquake sequence. *J Geophys Res Solid Earth* 90(B14):12691–12700
- Langer CJ, Hartzell S (1996) Rupture distribution of the 1977 western Argentina earthquake. *Phys Earth Planet Inter* 94:121–213
- Lay T, Wallace TC (1995) *Modern global seismology*. Elsevier, Amsterdam
- Lomnitz C (2012) *Seismic risk and engineering decisions*, vol 15. Elsevier, Amsterdam
- Rösler B, van der Lee S (2020) Using seismic source parameters to model frequency-dependent surface-wave radiation patterns. *Seismol Res Lett* 91:992–1002
- Sadigh K, Chang C, Egan J, Makdisi F, Youngs R (1997) Attenuation relationships for shallow crustal earthquakes based on California strong motion data. *Seism Res Lett* 68:180–189
- Sairam B, Rastogi BK, Aggarwal S, Chauhan M, Bhone U (2011) Seismic site characterization using VS30 and site amplification in Gandhinagar region, Gujarat, India. *Current Sci* 100:754–761
- Somerville PG, Smith NF, Graves RW, Abrahamson NA (1997) Modification of empirical strong ground motion attenuation relations to include the amplitude and duration effects of rupture directivity. *Seismol Res Lett* 68(1):199–222
- U.S. Geological Survey (2018) Earthquake catalog. <https://www.earthquake.usgs.gov/earthquakes/search/> Accessed 24 May 2018